

A Comparative Analysis of Spectral Reflectance Estimated in Various Spaces Using a Trichromatic Camera System

Francisco H. Imai[▲], Roy S. Berns[▲] and Di-Y. Tzeng^{▲*}

Munsell Color Science Laboratory, Chester F. Carlson Center for Imaging Science, Rochester Institute of Technology, Rochester, New York

Principal component analysis coupled with multi-channel digital image capture is a powerful technique for spectral scene estimation. Most often, the linear modeling is performed using a spectral reflectance factor. However, it is well known that for many subtractive coloration systems, spectral reflectance is nonlinearly related to colorant amount. Accordingly, the accuracy of spectral reconstruction has been evaluated as a function of the spectral definition of the ensemble. Specifically, Kubelka–Munk turbid media theory and a new empirical transformation, optimized for optimal data normality, were compared with spectral reflectance factor. Both tested spaces are nonlinear transformations of spectral reflectance factor. In addition, a new technique of multi-channel digital image capture was developed and tested. This technique combined trichromatic image capture with color filtration resulting in multiple signals in sets of three. Six eigenvectors based on the new empirical space coupled with digital capture with and without a light-blue absorption filter produced the most accurate spectral scene estimation from among the various tested combinations.

Journal of Imaging Science and Technology 44: 280–287 (2000)

Introduction

A digital image capturing system has been developed that potentially results in spectral image archives with sufficient spatial resolution and colorimetric accuracy for artwork imaging including internet display and multi-ink printing minimizing metamerism.^{1–5} In this system, a low-spatial resolution spectral image is combined with a high-spatial resolution lightness image (from either a monochrome digital camera or digitized photograph) to generate a high-spatial resolution spectral image. The advantages of this dual capture system are principally in reducing the cost and complexity of the image acquisition system compared with traditional high-resolution multi-spectral imaging systems. This method applies *a priori* spectral analysis, linear modeling techniques, and exploiting of the human visual system's spatial properties to achieve high-resolution multi-spectral images. Preliminary experiments using this method have shown promising results. Furthermore, a new technique of multi-spectral imaging combining trichromatic image capture with color filtration resulting in multiple signals in sets of three was developed and tested.⁴

Technical issues concerned with multi-spectral image acquisition have been studied extensively.^{1–20} Traditionally, the spectral reconstruction from digital camera signals has been performed in reflectance space, because digital camera signals are directly related to spectral reflectance factor. When dealing with

spaces other than reflectance, *e.g.* absorption, absorption vectors and digital count vectors are not in the same space and a non-linear transformation should be performed *a priori* to produce digital counts directly related to the space. This digital count transformation enables the use of principal component analysis and other linear modeling tools.

This article will analyze spectral reconstruction performed in spectral representations using transformed normalized signals from a trichromatic camera combined with absorption filters. These representations include reflectance factor, the opaque form of Kubelka–Munk turbid-media theory (K/S), and a new empirical transformation proposed by Tzeng²¹ that gives a near-normal and reduced dimensionality representation for subtractive opaque processes.

Theory of Spectral Reconstruction from Multiple Camera Signals

The spectral reflectance of each pixel of a painting can be estimated using *a priori* spectral analysis with direct measurement and imaging of color patches to establish a relationship between digital counts and spectral reflectance factor.

A set of sampled spectral reflectance with dimension $n \times 1$, \mathbf{r} , is measured, where n is the number of wavelength measurements. Using principal component analysis, the $n(n \times 1)$ eigenvectors $\{\mathbf{e}_1, \mathbf{e}_2, \dots, \mathbf{e}_n\}$ and the scalar eigenvalues $\{a_1, a_2, \dots, a_n\}$ associated with each eigenvector are calculated from the measured spectral reflectances. Arranging the eigenvalues in descending order, the fraction of variance explained by the first i vectors, also called the cumulative contribution index, is given by Eq. 1.

Invited paper; Original manuscript received December 15, 1999

Color Plates 1, 2, 3 and 4 are printed in the Color Plate Section of this issue, on pages 376 and 377.

▲ IS&T Member

* Current address: Applied Science Fiction, Austin, Texas

©2000, IS&T—The Society for Imaging Science and Technology

$$v_i = \frac{\sum_{k=1}^i a_k}{\sum_{k=1}^n a_k} \quad (1)$$

The cumulative contribution index v_i has been used to determine the appropriate number of basis vectors, i , to be used in the spectral reflectance estimation. The colorimetric and spectral accuracy of the spectral reflectance estimation also can be considered as selection criteria. The estimated spectral reflectance vector using i eigenvectors is given by Eq. 2.

$$\hat{\mathbf{r}} = \mathbf{E}_i \alpha_i \quad (2)$$

where $\mathbf{E}_i = [\mathbf{e}_1, \mathbf{e}_2, \dots, \mathbf{e}_i]$, and the coefficients are given by $\alpha_i = [a_1, a_2, \dots, a_i]^T$ where T denotes matrix transpose.

The camera digitizing system gives $m \times 1$ digital counts, \mathbf{C} , where m counts the number of camera channels. The number of channels, m , should be the same or larger than the number of eigenvectors i used in the spectral reflectance estimation. A relationship between digital counts, \mathbf{C} , and eigenvalues, α , can be established by Eq. 3.

$$\mathbf{A} = \alpha \mathbf{C}^T [\mathbf{C} \mathbf{C}^T]^{-1} \quad (3)$$

Equation 3 is the usual pseudo-inverse calculation.

The matrix \mathbf{A} can be used to estimate the eigenvalues, $\hat{\alpha}$, from digital counts, as shown in Eq. 4.

$$\hat{\alpha} = \mathbf{A} \mathbf{C} \quad (4)$$

Finally, combining Eqs. 2 and 4 it is possible to estimate the spectral reflectance vector from the multiple camera signals as shown in Eq. 5.

$$\hat{\mathbf{r}} = \mathbf{E} \mathbf{A} \mathbf{C} \quad (5)$$

Spaces to Perform Principal Component Analysis

Reflectance space, r_2 , is directly related to the digital counts of the camera system and it is traditionally used to perform spectral analysis. A digital camera with linear photometric response can be modeled using Eq. 6 to establish a relationship between camera digital counts, \mathbf{C} , and the object spectral reflectance, $\mathbf{r} = (r_1, r_2, \dots, r_n)^T$.

$$\mathbf{C} = (\mathbf{D} \mathbf{F})^T \mathbf{S} \mathbf{r} \quad (6)$$

where \mathbf{D} is a matrix with camera spectral sensitivities in its diagonal as shown in Eq. 7,

$$\mathbf{D} = \begin{pmatrix} d_1 & & & 0 \\ & d_2 & & \\ & & \ddots & \\ 0 & & & d_n \end{pmatrix}, \quad (7)$$

\mathbf{F} is a matrix with transmittance characteristics of the p filters in its columns as shown in Fig. 8,

$$\mathbf{F} = \begin{pmatrix} f_{1,1} & f_{1,2} & \cdots & f_{1,p} \\ \vdots & \vdots & \cdots & \vdots \\ f_{n,1} & f_{n,2} & \cdots & f_{n,p} \end{pmatrix} \quad (8)$$

and \mathbf{S} is the matrix with the sampled illumination spectral power distribution in the diagonal as shown in Fig. 9.

$$\mathbf{S} = \begin{pmatrix} s_1 & & & 0 \\ & s_2 & & \\ & & \ddots & \\ 0 & & & s_n \end{pmatrix}, \quad (9)$$

Alternative spaces can also be used to perform spectral reconstruction.

Kubelka–Munk Space. Reflection, absorption and scattering occur when opaque surfaces are exposed to light. Kubelka and Munk proposed a turbid media theory that derived the relationship between reflectance factor, absorption, and scattering based on a simplifying assumption that flux within an absorbing and scattering layer only travels in two fluxes perpendicular to the layer.²² According to the Kubelka–Munk formulation, reflectance factor is a function of a absorption, K , and scattering, S , ratio. The Kubelka–Munk equations relating reflectance factor, R_λ , and the ratio, $(K/S)_\lambda$, for opaque materials are given by Eqs. 10 and 11.

$$R_\lambda = 1 + (K/S)_\lambda - \sqrt{(K/S)_\lambda ((K/S)_\lambda + 2)} \quad (10)$$

$$(K/S)_\lambda = \frac{(1 - R_\lambda)^2}{2R_\lambda} \quad (11)$$

Thus, $(K/S)_\lambda$ is a function of reflectance factor, shown in Eq. 12.

$$\Phi = f(\mathbf{r}) \quad (12)$$

where Φ is a vector representing the $(K/S)_\lambda$ ratio, after the convention of Allen²³ and Berns.²⁴

In Kubelka–Munk space the ratio $(K/S)_\lambda$ of absorption and scattering is approximately linear²⁵ with respect to colorant concentration as shown in Eq. 13.

$$\Phi = \phi \mathbf{c} \quad (13)$$

where \mathbf{c} is the vector of concentration and ϕ is the basis functions [often their $(K/S)_\lambda$ at unit concentration] of a set of colorants. Therefore, the absorption and scattering properties of materials also provide a useful way to perform color analysis. The linear relation has been used successfully in the prediction of paints, plastics, textiles, etc. Intuitively, Kubelka–Munk space, Φ , is expected to perform better than reflectance space, \mathbf{r} , that is nonlinear to colorant amount in subtractive color systems.²⁴

New Empirical Space. Spectral reconstruction using Φ space sometimes results in large errors for light colors.²¹ This is caused by errors of spectral estimation in low dimensionality that can produce negative values inside the square root of Eq. 10, and implies that the set of eigenvectors do not span sufficient spectral variance and are not of sufficient normality for accurate reconstruction. In multivariate analyses,²⁶ techniques are available for evaluating normality, as well as deriving empirical transformations which minimize reconstruction errors, such as those found with Φ space.

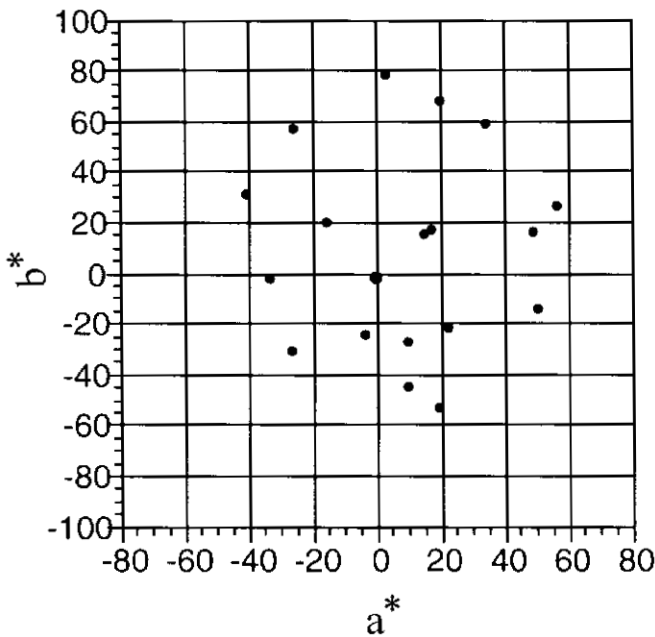


Figure 1. a^*b^* distribution plot of GretagMacbeth ColorChecker for illuminant D50 and 2° observer.

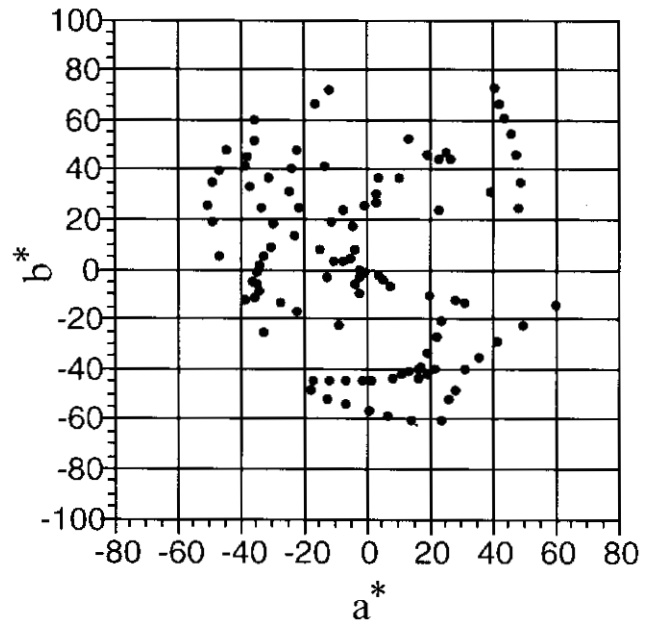


Figure 2. a^*b^* distribution plot of 105 poster-color painted patches for illuminant D50 and 2° observer.

Tzeng²¹ used the transformations shown in Eqs. 14 and 15 with good success.

$$R_\lambda = (a_\lambda - \Psi_\lambda)^2 \quad (14)$$

$$\Psi_\lambda = a_\lambda - \sqrt{R_\lambda} \quad (15)$$

where a_λ is an offset vector, which is empirically derived by optimization tools and Ψ_λ is the notation for the new empirical space.

The use of the square root transformation of the spectral reflectance improves normality and the offset term is required to account for a subtractive opaque colorant formulation. The new empirical space, Ψ , is approximately linear²¹ with respect to colorant concentration as shown in Eq. 16.

$$\Psi = \psi C \quad (16)$$

where c is the vector of concentration and ψ is the basis function of a set of colorants.

Transformation of Digital Counts in Kubelka-Munk and New Empirical Spaces. A digital camera with a linear photometric response produces digital counts, C , that do not have direct proportionality with Kubelka-Munk and the new empirical spaces. In order to solve this problem, transformations for the digital counts were derived, in the same way as defined in Eqs. 11 and 15 and described by Eqs. 17 and 18 for Kubelka-Munk and the new empirical spaces, respectively.

$$C' = \frac{1}{2C} + \frac{C}{2} - 1 \quad (17)$$

$$C' = 1 - \sqrt{C}, \quad (18)$$

where C' is the transformed digital count.

The effectiveness of the corrections given by Eqs. 17 and 18 in a system without camera noise were tested by simulating camera signals defined by Eq. 6. As a result of the simulation, it was possible to observe that the non-linear transformations given by Eqs. 17 and 18 improved the accuracy of the spectral estimation.⁵

Experimental

In our experiments, we considered two targets captured using combinations of trichromatic signals from a digital camera system to compare the spectral reflectance estimation performed in three different spaces.

A GretagMacbeth ColorChecker and a set of 105 painted patches were imaged. The ColorChecker was used due to its familiarity to imaging professionals as well as giving a basis for comparison. The painted patches were produced using poster-color paints (Cerulean Blue and Rose Violet manufactured by Sakura; Ultramarine, Permanent Yellow, Sap Green and Black manufactured by Pentel). The patches produced using the poster-color paints were coated with Krylon Kamar Varnish that is a non-yellowing protection.

The spectral reflectances of the ColorChecker were measured in wavelength intervals of 10 nm from 400nm to 700nm using the Macbeth ColorEye 7000 spectrophotometer with integration sphere (specular included, UV excluded). The painted patches were measured in wavelength intervals of 10 nm from 400 nm to 700 nm using a Gretag SPM60 45/0 spectrophotometer.

The distribution of the CIELAB coordinates for the GretagMacbeth ColorChecker for illuminant D50 and the 2° observer projected onto the a^*b^* plane is shown in Fig. 1. The distribution of the 105 poster-color painted patches is shown in Fig. 2.

For the imaging system, we used a high-resolution IBM PRO3000 digital camera system ($3,072 \times 4,096$ pixels, 12 bits per channel). More details of the image capture system can be found in Ref. 27. A Kodak Wratten light-blue absorption filter number 38 was used to give trichromatic signals that were coupled with the trichromatic signals of

TABLE I. Influence of the number of eigenvectors in each space used in the spectral reconstruction on the colorimetric and spectral error for Gretag Macbeth ColorChecker. The table shows mean color difference in ΔE^*_{94} , mean metamerism index (M.I.) in ΔE^*_{94} comparing illuminants D50 and A for 1931 observer, and the reflectance factor rms error.

Dimension	Reflectance Space r			Kubelka–Munk space Φ			New Empirical Space Ψ		
	Mean ΔE^*_{94} (1931, D50)	Mean M.I. D50, A ΔE^*_{94}	Reflectance factor rms error	Mean ΔE^*_{94} (1931, D50)	Mean M.I. D50, A ΔE^*_{94}	Reflectance factor rms error	Mean ΔE^*_{94} (1931, D50)	Mean M.I. D50, A ΔE^*_{94}	Reflectance factor rms error
3	2.9	1.4	0.032	4.1	1.3	0.010	2.5	1.1	0.025
6	0.3	0.2	0.013	1.4	0.8	0.039	0.2	0.1	0.009
9	0.2	0.07	0.007	0.3	0.1	0.027	0.08	0.03	0.004
12	0.02	0.01	0.002	0.2	0.1	0.017	0.01	0.01	0.001

TABLE II. Influence of the number of eigenvectors in each space used in the spectral reconstruction on the colorimetric and spectral error for 105 poster-color painted patches. The table shows mean color difference in ΔE^*_{94} , mean metamerism index (M.I.) in ΔE^*_{94} comparing illuminants D50 and A for 1931 observer, and the reflectance factor rms error.

Dimension	Reflectance Space r			Kubelka–Munk space Φ			New Empirical Space Ψ		
	Mean ΔE^*_{94} (1931, D50)	Mean M.I. D50, A ΔE^*_{94}	Reflectance factor rms error	Mean ΔE^*_{94} (1931, D50)	Mean M.I. D50, A ΔE^*_{94}	Reflectance factor rms error	Mean ΔE^*_{94} (1931, D50)	Mean M.I. D50, A ΔE^*_{94}	Reflectance factor rms error
3	3.6	2.3	0.027	3.7	3.0	0.020	1.9	1.5	0.019
6	1.2	0.5	0.010	0.9	0.5	0.022	0.5	0.3	0.006
9	0.06	0.04	0.002	0.4	0.2	0.019	0.06	0.03	0.002
12	0.04	0.02	0.001	0.05	0.03	0.005	0.01	0.01	0

the camera without absorption filter, in order to produce six channels.*

Results and Discussion

Performance of Principal Component Analysis in Different Spaces. The technique for spectral reflectance estimation is based on *a priori* spectral analysis and principal component analysis. Thus, it was of interest to evaluate the spectral reconstruction accuracy of principal component analysis in each of three spaces considered, r , Φ , Ψ .

Table I shows the influence of the number of eigenvectors on the colorimetric and spectral accuracy of the estimation for the GretagMacbeth ColorChecker. Table II shows the influence of the number of eigenvectors on the colorimetric and spectral accuracy of 105 patches produced using mixtures of poster-color paints. The color difference calculations in ΔE^*_{94} were performed for illuminant D50 and the 2° observer. The metamerism index was calculated using the Fairman metamerism black method, between standard illuminants D50 and A using ΔE^*_{94} in the calculations.²⁸ The number of eigenvectors corresponding to the dimension of the spectral estimation is presented in multiples of three because we are considering multiple sets of trichromatic signals for the spectral estimation.

Tables I and II show that six eigenvectors and as a consequence, six channels is a compromise between accuracy and the cost of adding more sets of trichromatic channels.

Analyzing the overall reconstruction results of the targets, the spectral estimation in the new empirical space presented the best colorimetric and spectral accuracy. The spectral estimation in reflectance space presented slightly worse spectral and colorimetric accuracy than the reconstruction in the new empirical space and the spectral estimation in Kubelka–Munk space presented the worst performance except for poster-color painted patches estimation using 6 eigenvectors.

Figures 3, 4, and 5 show the ΔE^*_{94} histogram comparing the measured and predicted spectral reflectances of 105 painted patches using principal components, respectively in reflectance, Kubelka–Munk and the new empirical spaces. Figure 4 shows that almost half of the samples have ΔE^*_{94} less than 0.5 which explains why the spectral estimation in Kubelka–Munk spaces has, in general, better results than the spectral estimation in reflectance space, as indicated by the broad distribution of Fig. 3. These histograms further explain why the spectral estimation in Kubelka–Munk space resulted in smaller mean ΔE^*_{94} than the spectral estimation in reflectance space for the poster-color paints using 6 eigenvectors. However, as also shown in Fig. 4, the spectral estimation in Kubelka–Munk space produced large color differences corresponding to patches with light colors.

Figure 5 shows that most of the samples have the spectral reflectance estimated in the new empirical space with color difference less than 1 ΔE^*_{94} units.

Color Plates 1, 2, and 3 (pp. 376–377) show the normal plot, respectively for reflectance factor, Kubelka–Munk coefficients, and new empirical space coefficients generated using MATLAB statistical tool.²¹ If the normal plot at each sampled wavelength is a straight line the distribution is normal and the non-normal distribution reveals curvature in the normal plot.

The normal plot of the samples in new empirical space presented less deviation from straight lines than the normal plot in Kubelka–Munk space and the normal plot

* Several different filters such as didymium and Kodak Wratten no. 66 were evaluated with similar results. This evaluation included both simulations to alleviate capture noise and actual measurements. Although the choice of filter can be critical, no significant differences were observed in the performance using Kodak Wratten nos. 38, 66 and a didymium filter. The light-blue filter was chosen because it provided the best performance. A filter optimization should be performed in future research.

TABLE III. Spectral estimation accuracy of Gretag Macbeth ColorChecker using 6 eigenvectors in new empirical space for 6 measured signals: R, G, B without filter and R, G, B with Kodak Wratten absorption filter number 38 (light-blue).

Results	ΔE_{ab}^* (D50, 2°)	ΔE_{94}^* (D50, 2°)	Reflectance factor rms error	Metameric index (ΔE_{94}^*) (D50, A)
Mean	2.9	1.9	0.029	0.8
Standard Deviation	1.8	0.9	0.013	0.5
Max	7.5	3.5	0.066	2.0
Min	0.5	0.6	0.005	0.1

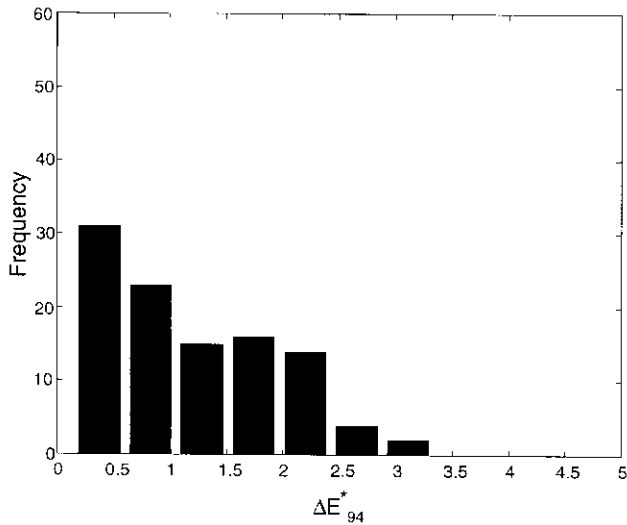


Figure 3. ΔE_{94}^* histogram of color difference between measured spectral reflectances of 105 poster-color painted patches and their spectral estimation using 6 eigenvectors in reflectance space for illuminant D50 and 2° observer.

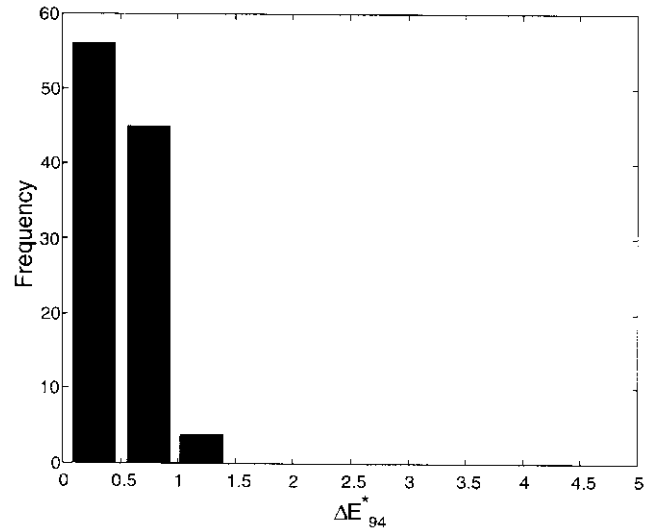


Figure 5. ΔE_{94}^* histogram of color difference between measured spectral reflectances of 105 poster-color painted patches and their spectral estimation using 6 eigenvectors in new empirical space for illuminant D50 and 2° observer.

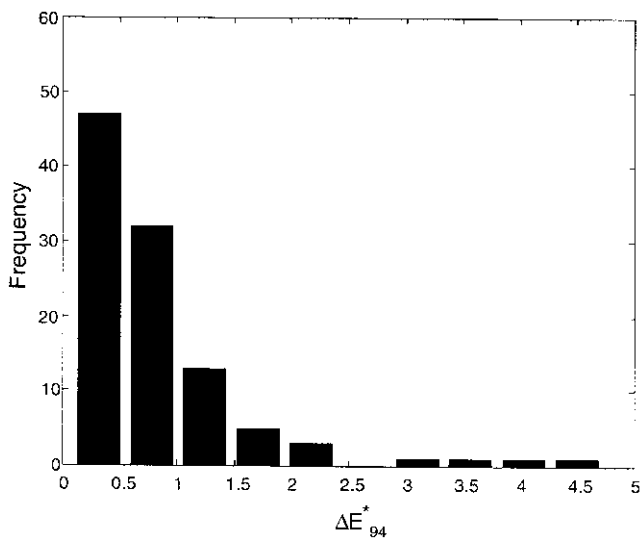


Figure 4. ΔE_{94}^* histogram of color difference between measured spectral reflectances of 105 poster-color painted patches and their spectral estimation using 6 eigenvectors in Kubelka-Munk space for illuminant D50 and 2° observer.

in Kubelka–Munk space showed less deviation from straight lines than the normal plot in reflectance space. The normal plots of Color Plates 1, 2, and 3 (pp. 370–371) well correlate with Table II and Figs. 3, 4, and 5.

The normal plot explains the better performance in terms of mean ΔE_{94}^* for 6 dimensions (channels, eigenvectors) of Kubelka–Munk space than the colorimetric performance in reflectance space shown in Table II. However, in terms of overall performance, the spectral estimation in reflectance space performs better than Kubelka–Munk space because the simulations in Kubelka–Munk space produced spectral mismatches and large colorimetric errors for patches with high reflectance factors. High reflectance factors produce very small (K/S) values. When spectral reconstruction is performed using principal component analysis in reduced dimensionality there is an error in the reconstruction that can produce negative (K/S) values. When these negative values are introduced in Eq. 10 we have negative values under a radical. For example, Fig. 6 shows the comparison of the measured and estimated spectral reflectance of the Orange-Yellow patch of the GretagMacbeth ColorChecker reproduced using six eigenvectors in Kubelka–Munk space. It shows a considerable mismatch in the high reflectance factor region of the spectrum. However, the estimation in Kubelka–Munk space produced very good results for some patches with low reflectance factors, that was not reproduced so well in reflectance space, such as the purple patch of the GretagMacbeth ColorChecker. Figure 7 shows the comparison of the measured and estimated spectral reflectance of the purple patch reproduced using 6 eigenvectors in reflectance space. Figure 8 shows the comparison of the measured and estimated spectral re-

TABLE IV. Spectral estimation accuracy of 105 poster-color painted patches using 6 eigenvectors in new empirical space for 6 measured signals: R, G, B without filter and R, G, B with Kodak Wratten absorption filter number 38 (light-blue).

Results	ΔE^*_{ab} (D50, 2°)	ΔE^*_{94} (D50, 2°)	Reflectance factor rms error	Metameric index (ΔE^*_{94}) (D50, A)
Mean	2.1	1.2	0.017	0.9
Standard Deviation	1.1	0.6	0.008	0.6
Max	5.9	3.6	0.041	3.8
Min	0.1	0.1	0.005	0.1

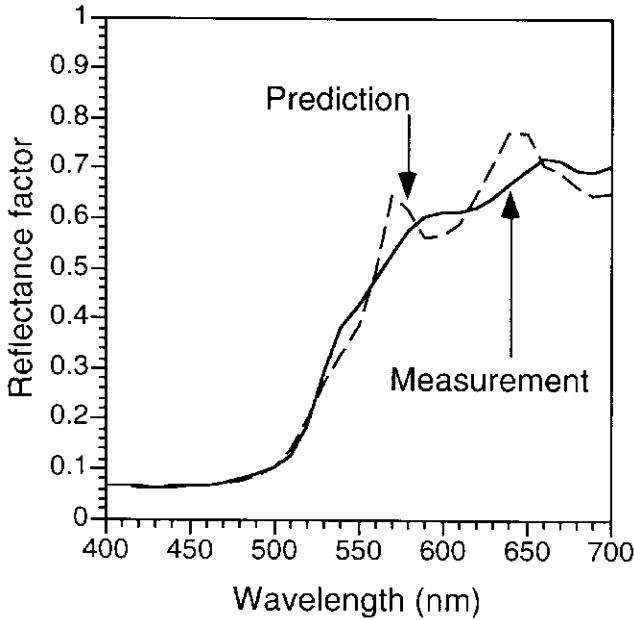


Figure 6. Comparisons of measured and predicted spectral reflectances of GretagMacbeth ColorChecker orange-yellow patch in Kubelka–Munk space using 6 eigenvectors.

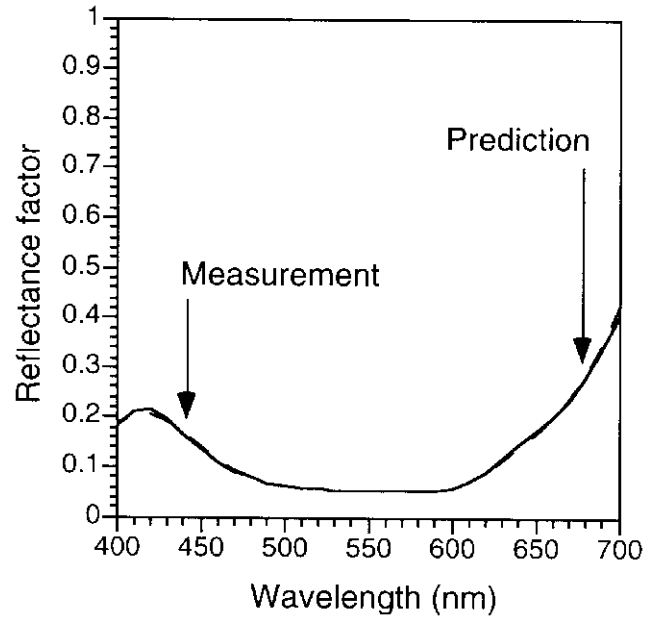


Figure 8. Comparisons of measured and predicted spectral reflectances of GretagMacbeth ColorChecker purple patch in Kubelka–Munk space using 6 eigenvectors.

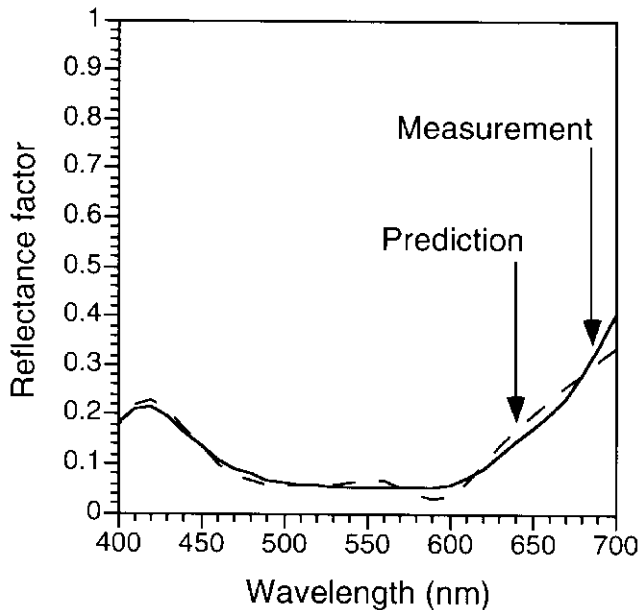


Figure 7. Comparisons of measured and predicted spectral reflectances of GretagMacbeth ColorChecker purple patch in reflectance space using 6 eigenvectors.

flectance of the purple patch reproduced using 6 eigenvectors in Kubelka–Munk space. These results show that although the spectral estimation in Kubelka–Munk space produces unacceptable inaccuracies for light colors it can produce better results than the spectral estimation in reflectance space for dark colors.

Estimation of Spectral Reflectance Using Measured Digital Counts

In this estimation, spectral reflectance is estimated from actually measured digital counts averaged over each imaged patch. Tables III and IV show the colorimetric and spectral accuracy for spectral estimation in the new empirical space, respectively, for the GretagMacbeth ColorChecker, and the poster-color painted patches.

Figures 9 and 10 show the ΔE^*_{94} histogram with comparison between the measured and predicted spectral reflectances of 105 poster-color painted patches in new empirical space, respectively, from simulated digital counts and actual digital counts. The digital counts were simulated using Eq. 6 and the measured camera spectral sensitivities, the measured spectral radiance of the illuminants of the IBM PRO/3000 digital camera system and the measured spectral transmittance of Kodak Wratten filter number 38 (light-blue).

Comparing the histograms of Figs. 9 and 10, the spectral estimation from actual digital counts were worse

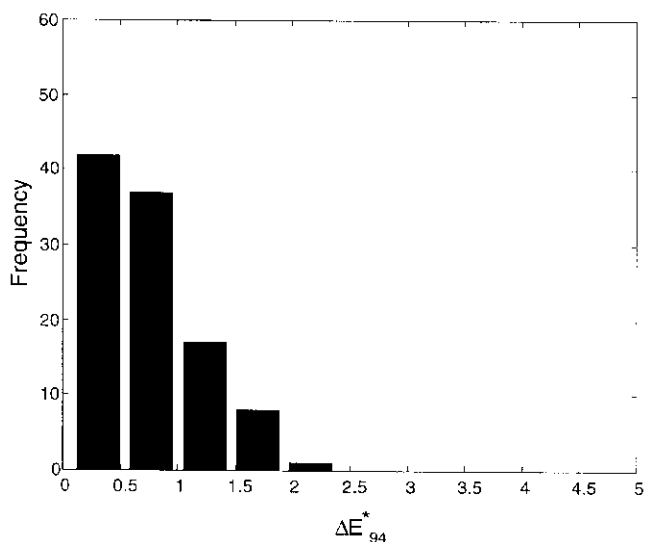


Figure 9. ΔE^*_{94} histogram of color difference between measured spectral reflectances of 105 poster-color painted patches and their spectral estimation using 6 simulated digital counts in new empirical space and 6 eigenvectors for illuminant D50 and 2° observer.

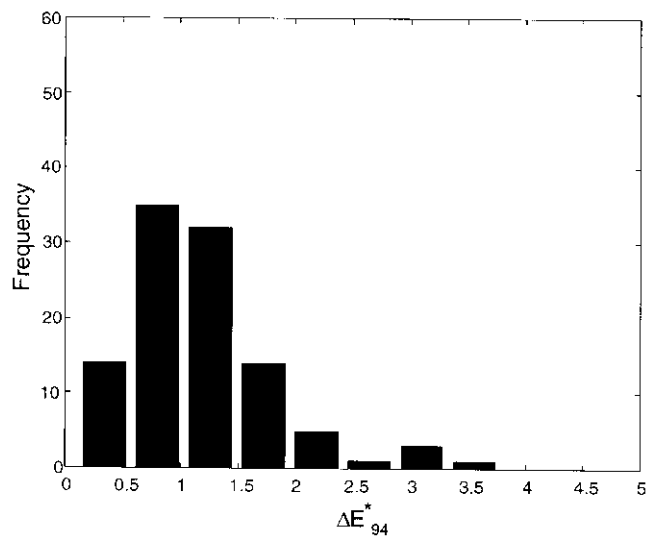


Figure 10. ΔE^*_{94} histogram of color difference between measured spectral reflectances of 105 poster-color painted patches and their spectral estimation using 6 actual measured digital counts and 6 eigenvectors in new empirical space for illuminant D50 and 2° observer.

than the spectral estimation based on simulated digital counts. This result was expected because of the introduction of noise and typical experimental error. However, the results we obtained for the spectral reconstruction of the GretagMachbeth ColorChecker with color difference ΔE^*_{ab} of 2.9 is better than the average ΔE^*_{ab} of 4.0, obtained using a monochrome digital camera and a set of 7 interference filters by Burns.¹⁹ Our results are also similar to the ΔE^*_{ab} between 2 and 3 (depending on the lighting used to image) obtained by the MARC camera in the VASARI project (though this system was optimized for colorimetric performance and does not estimate spectral data).²⁹

Color Plate 4 (p. 377) shows a comparison between measured poster-color painted patch spectral reflectance and the predictions of the spectral reflectance by principal component analysis, simulated digital counts and actual digital counts using 6 eigenvectors in the new empirical space. It is possible to notice that while the prediction by principal component analysis closely matches the measured spectral reflectance, the predictions by simulated digital counts and actual digital counts, progressively diverged from the measured spectral reflectance as we add noise from the imaging system.

Conclusions

The experimental sequence of the spectral reconstruction from trichromatic digital camera combined with absorption filters was described, showing, at first, the colorimetric and spectral accuracy predicted by statistical analysis of samples, and progressively adding noise, using measured digital counts from imaged patches. As a result, the spectral reconstruction using a combination of trichromatic signals without filtering and with light blue absorption filter coupled to the eigenvectors in the new empirical space produced the best overall colorimetric and spectral performance for the targets we analyzed. Spectral reconstruction using higher order estimation could produce better results. However, six eigenvectors in the empirical space presents a com-

promise between accuracy and fulfillment of our goals of simplicity and cost reduction. Furthermore, the average colorimetric result of our reconstruction for the GretagMachbeth ColorChecker was better or similar to other spectral reconstruction systems using traditional techniques with the advantage of simplifying the imaging system.

Although spectral estimation in Kubelka–Munk (K/S) space produced suitable spectral matches for colorants with low reflectance factors, it can produce unacceptable errors when reducing the dimensionality in principal component analysis. Therefore, this space is not recommended for the spectral estimation of artwork images unless iterative methods are incorporated (*e.g.* Refs. 30 and 31). \blacktriangle

References

1. F. H. Imai and R. S. Berns, High-resolution multi-spectral image archives: A hybrid approach, in *IS&T/SID Sixth Color Imaging Conference: Color Science, Systems, and Applications*, IS&T, Springfield, VA, 1998, pp. 224–227.
2. R. S. Berns, F. H. Imai, P. D. Burns and Di-Y. Tzeng, Multi-spectral-based color reproduction research at the Munsell Color Science Laboratory, *Proc. SPIE* **3409**, 14–25 (1998).
3. R. S. Berns, Challenges for color science in multimedia imaging, in L. MacDonald and M. R. Luo, Eds., *Colour Imaging: Vision and Technology*, John Wiley & Sons, Chichester, 1998, pp. 99–127.
4. F. H. Imai and R. S. Berns, Spectral Estimation Using Trichromatic Digital Cameras, in *International Symposium on Multispectral Imaging and Color Reproduction for Digital Archives*, 1999, pp. 42–49.
5. F. H. Imai and R. S. Berns, A comparative analysis of spectral reflectance reconstruction in various spaces using a trichromatic camera system, in *IS&T/SID Seventh Color Imaging Conference: Color Science, Systems, and Applications*, IS&T, Springfield, VA, 1999, pp. 21–25.
6. J. Y. Hardeberg, H. Brettel, and F. Schmitt, Spectral characterization of electronic cameras, *Proc. SPIE* **3409**, 100–109 (1998).
7. H. Maitre, F. J. M. Schmitt, J-P. Crettez, Y. Wu and J. Y. Hardeberg, Spectrophotometric image analysis of fine art paintings, in *IS&T/SID Fourth Color Imaging Conference: Color Science, Systems, and Applications*, IS&T, Springfield, VA, 1996, pp. 50–53.
8. S. Baronti, A. Casini, F. Lotti and S. Porcinai, Multispectral imaging system for the mapping of pigments in works of art by use of principal-component analysis, *Appl. Opt.* **37**, 1229–1309 (1998).

9. F. König, Reconstruction of natural spectra from a color sensor using nonlinear estimation methods, in *IS&T's 50th Annual Conference*, IS&T, Springfield, VA, 1997, pp. 454–458.
10. F. König and W. Præfke, The practice of multispectral image acquisition, in *Electronic Imaging: Processing, Printing, and Publishing in Color*, Jan Bares, Ed., *Proc. SPIE* **3409**, 34–41 (1998).
11. W. Præfke, Analysis-synthesis transforms versus orthogonal transforms for coding reflectance spectra, in *IS&T/SID Fifth Color Imaging Conference: Color Science, Systems, and Applications*, IS&T, Springfield, VA, 1997, pp. 177–181.
12. W. Præfke, Transform coding of reflectances spectra using smooth basis vectors, *J. Imaging Sci. Technol.* **40**, 543–548 (1996).
13. Y. Miyake, Y. Yokoyama, N. Tsumura, H. Haneishi, K. Miyata and J. Hayashi, Development of multiband color imaging systems for recording of art paintings, *Proc. SPIE* **3648**, 218–225 (1999).
14. H. Haneishi, T. Hasegawa, N. Tsumura and Y. Miyake, Design of color filters for recording artworks, in *IS&T's 50th Annual Conference*, IS&T, Springfield, VA, 1997, pp. 369–372.
15. S. Tominaga, Spectral Imaging by a Multi-Channel Camera, *Proc. SPIE* **3648**, 38–47 (1999).
16. M. J. Vrhel and H. J. Trussel, Color correction using principal components, *Color Res. Appl.* **17**, 328–338 (1992).
17. M. J. Vrhel, R. Gershon and L. S. Iwan, Measurement and analysis of object reflectance spectra, *Color Res. Appl.* **19**, 4–9 (1994).
18. D. S. S. Vent, *Multichannel analysis of object-color spectra*, M.S. Thesis, Rochester Institute of Technology, Rochester, NY, 1994.
19. P. D., Burns, *Analysis of image noise in multi-spectral color acquisition*, Ph. D. Thesis, Rochester Institute of Technology, Rochester, NY, 1997.
20. P. D. Burns and R. S. Berns, Error propagation analysis in color measurement and imaging, *Color Res. Appl.* **22**, 280–289, (1997).
21. D-Y. Tzeng, Spectral-based color separation algorithm development, Ph. D. Thesis, Rochester Institute of Technology, Rochester, NY, 1999.
22. P. Kubelka, and F. Munk, Ein Beitrag zur Optik der Farbenstriche, *Z. Tech. Phys.* **12**, 593–601 (1931).
23. E. Allen, Colorant Formation and Shading, in *Optical Radiation Measurements*, Vol. 2, *Color Measurment*, F. Grum and C. J. Bartleson, Eds., Academic Press, New York, 1980, pp. 290–336.
24. R. S. Berns, A Generic Approach To Color Modeling, *Color Res. Appl.* **22**, 318–325, (1997).
25. E. Allen, Basic equation used in computer color matching, *J. Opt. Soc. Am.* **56**, 1256–1259 (1966).
26. R. A. Johnson and D. W. Wichern, *Applied Multivariate Statistical Analysis*, 3rd ed., Prentice Hall, New Jersey, 1992.
27. F. H. Imai, Multi-spectral Image Acquisition and Spectral Reconstruction using a Trichromatic Digital Camera System Associated with Absorption Filters, Munsell Color Science Laboratory Technical Report, Rochester, NY, 1998, <http://www.cis.rit.edu/research/mcsl/pubs/PDFs/CameraReport.pdf>.
28. H. S. Fairman, Metameric correction using parameric decomposition, *Color Res. Appl.*, **12**, 261–265 (1997).
29. J. Cupitt, D. Saunders and K. Martinez, Digital imaging in European museums, *Proc. SPIE* **3025**, 144–151 (1997).
30. M. A. Rodriguez and T. G. Stockham, Producing colorimetric data from densitometric scans, *Proc. SPIE* **1913**, 413–418 (1993).
31. R. S. Berns and M. J. Shyu, Colorimetric characterization of a desktop drum scanner using a spectral model, *J. Electron. Imag.* **4**, 360–372 (1995).

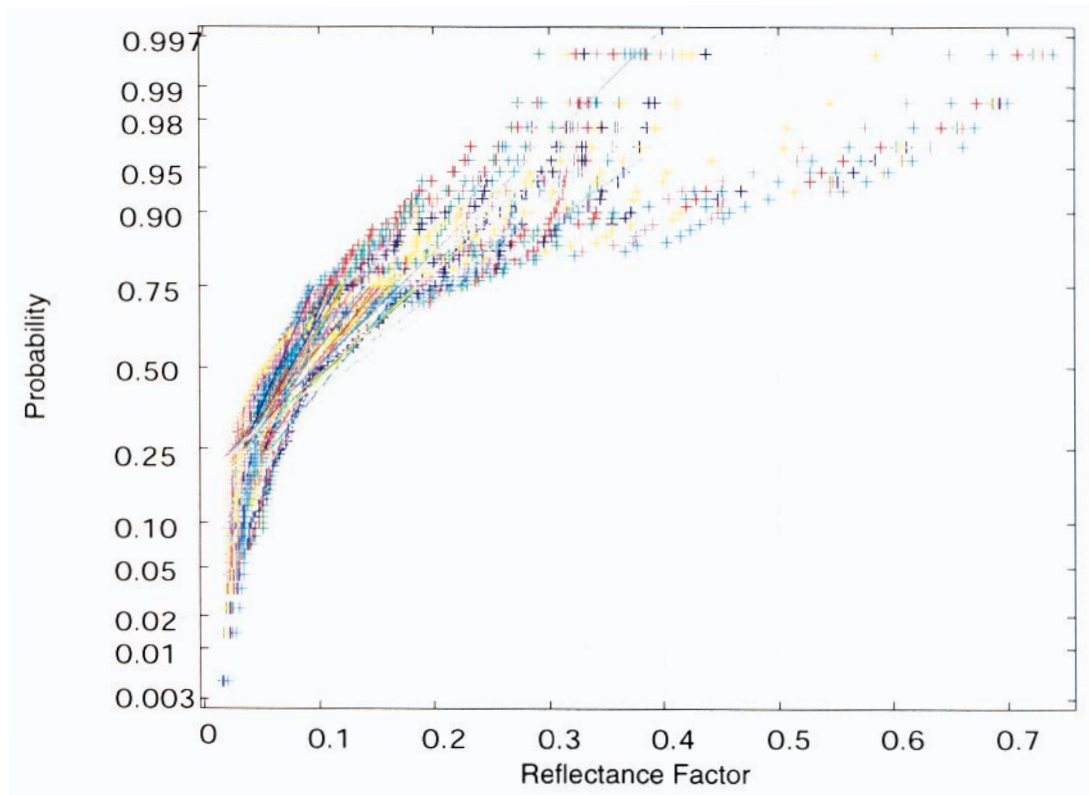


Plate 1. Normal probability plot of reflectance factors for 105 poster-color painted patches (Imai, *et al.*, pp. 280–287).

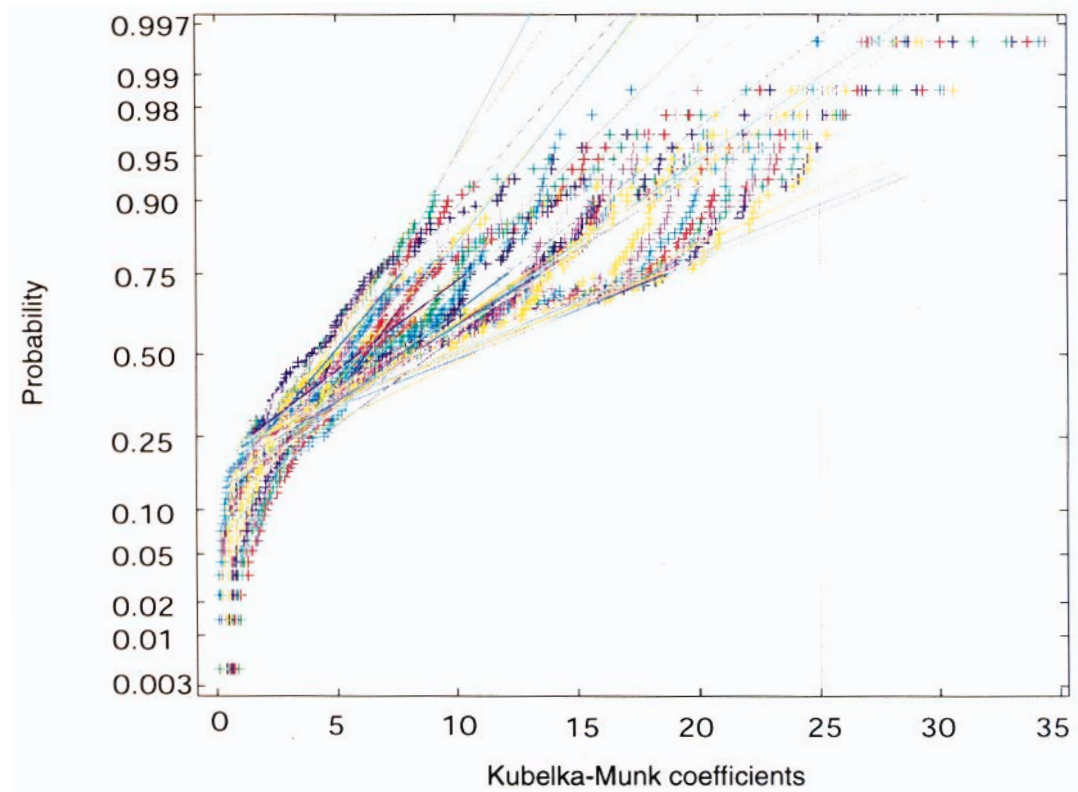


Plate 2. Normal probability plot of Kubelka–Munk coefficients for 105 poster-color painted patches (Imai, *et al.*, pp. 280–287).

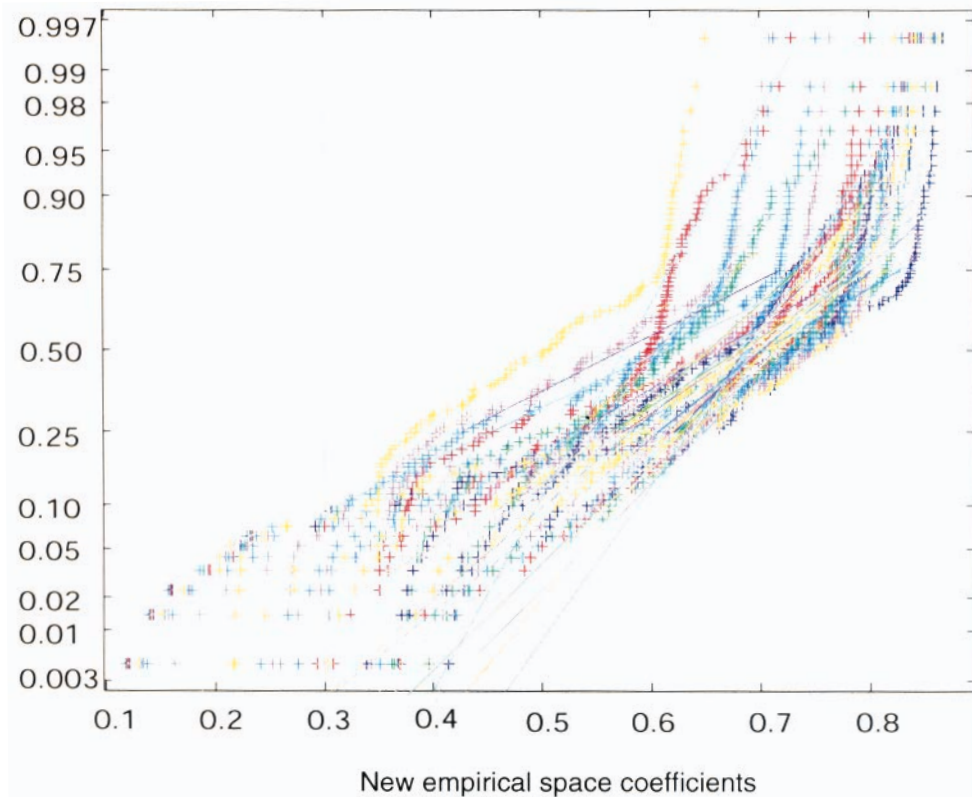


Plate 3. Normal probability plot of new empirical space coefficients for 105 poster-color painted patches (Imai, *et al.*, pp. 280–287).

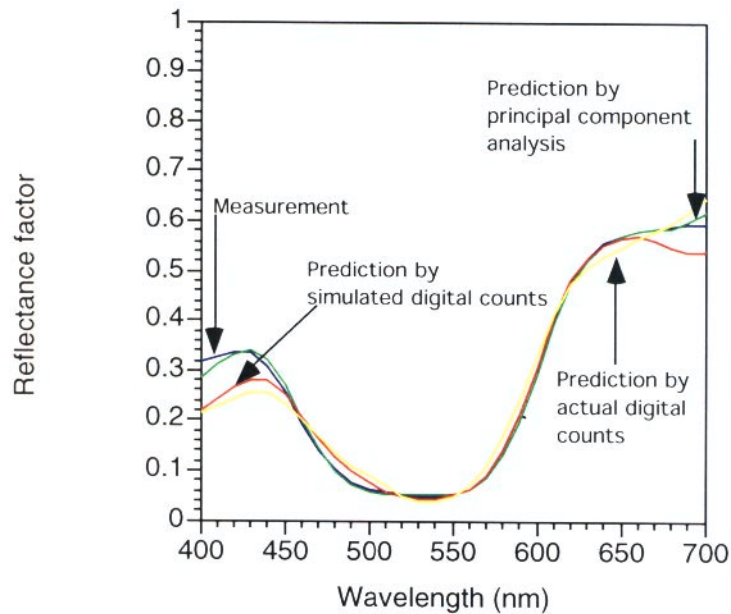


Plate 4. Comparison between measured poster-color painted patch spectral reflectance and the predictions of the spectral reflectance by principal component analysis, simulated digital counts and actual digital counts using 6 eigenvectors in new empirical space. The trichromatic capture combined the digital counts without filter and using Kodak Wratten filter number 38 to acquire 6 channels (Imai, *et al.*, pp. 280–287).